Soils and Rocks
An International Journal of Geotechnical and Geoenvironmental Engineering
www.soilsandrocks.com
ISSN 1980-9743
ISSN-e 2675-5475

Experimental and numerical analysis of instrumented caissons in tropical soil

Regina Maria Ferreira[1#], Paulo José Rocha de Albuquerque[1], Neusa Maria Bezerra Mota[2]

Case Study

Keywords:
Caisson
Numerical analysis
Load-settlement
Static load test

Abstract

This paper presents an experimental and numerical study on the behavior of three (3) instrumented caissons in a tropical laterite soil in the Planalto Central, DF, Brazil. The concrete caissons have a shaft diameter of 0.6 m, a bell diameter of 1.2 m and 1.3 m and lengths of 8.9 to 14.4 m. Static load tests were conducted out to investigate the behavior of the caissons. The results of load vs displacement and their interactions with the tropical soil were measured and evaluated using the methodology of Camapum de Carvalho et al. (2008, 2010) and numerical modeling with back-calculation of static load tests in the Plaxis 3D software. The paper presents the analysis of the load transfer lines and the comparison with the proposed methods. The results pointed to a constant load transfer along the shaft, with a significant contribution from the skin friction, developed for a fraction of the displacement necessary for its mobilization. The accuracy of using the Camapum de Carvalho et al. methodology stands out (2008, 2010), identifying the region dominated by skin friction, tip and plasticization of the foundation, confirming the authors' predictions for a tropical soil in the Distrito Federal/DF, Brazil. The numerical method using the Plaxis 3D software, proves that for the limit test load there was a significant contribution from skin friction, which must be consider in the analysis of the behaviour of caissons.

1. Introduction

In foundation engineering, when there is a need to design a construction with the transmission of high loads to the substrate, it is necessary to use deep foundations such as displacement piles, bored piles, caissons, and micro-piles. These types of piles are current standards for deep foundations, especially when to support high loads. The caisson is a special type of deep foundation, with a load capacity increase system obtained through the widening of the bell and one of the most important aspects is the understanding of its behavior when subjected to high compression loads. According to Berberian (2017), in Brazil caisson is used in many works, mainly due to aspects of geotechnical performance, as it is an alternative foundation with the possibility of using light equipment, and in porous soil it is easy to excavate and stable in vertical cuts. Such advantages are possible due to the stability of the excavations and the absence of ground water. However, even with the significant amount of work carried out on caissons, there is little studies on behavior through instrumented static load tests and numerical modeling. This occurs due to the peculiarity of this type of foundation, since the mobilization of skin friction is developed from small displacements, which can cause an excess of load on the shaft before this load can be transferred to the bell.

According to Brown et al. (2018); Das (2016); Herrmann et al. (2013), Murthy (2002); Bowles (1997) and Johnson et al. (1981), the execution of foundations in caissons has the main advantages: greater load capacity concentrated in a single caisson; enable changes to design criteria during excavation, depending on the type of soil found; possibility of direct inspection of the bearing capacity of the soil and the foundation where the base will be laid; easy construction in cohesive soils and rock mass, without deflection of the shaft; suitability in distinct types of soil; visual inspection of the shaft material so that the nature of the substrate can be confirmed; possibility of extremely high resistance; ease of increasing the shaft to allow greater bending moments; low noise and vibration level; reduction in the number of piles excavated under concentrated loads and can be easily adjusted to accommodate variable conditions encountered during its execution.

To understand the compression behavior of caissons built in a tropical laterite soil in the Planalto Central, DF, Brazil, based on static load tests, Camapum de Carvalho et al. (2008, 2010) proposed a methodology considering the characteristic

[#]Corresponding author. E-mail address: regina.marya@hotmail.com
[1]Universidade Estadual de Campinas, Faculdade de Engenharia Civil, Arquitetura e Urbanismo, Campinas, SP, Brasil.
[2]Universidade do Porto, Faculdade de Engenharia, Porto, Portugal.

Submitted on October 9, 2023; Final Acceptance on August 10, 2024; Discussion open until February 28, 2025.

https://doi.org/10.28927/SR.2024.010223

behavior of each soil and its interaction mechanisms between the foundation elements. It is a valuable tool for analyzing load tests, without instrumentation along the shaft. Silva (2011) and Castro Neto et al. (2019), applied the aforementioned methodology to tropical soil, validating the predictions obtained from the method. For numerical simulations in the Plaxis 3D software, the initial model validation procedure was based on back-calculation, based on empirical correlations of soil parameters, of data obtained from the Standard Penetration Test (SPT), making a variation of these parameters in the input data of the software, until the load vs displacement curve shows the same behavior as the static load tests.

According to Albuquerque (2001), it is difficult to understand and complex to understand the load distribution mechanism in foundations. According to the author, the evaluation of the tip load and distribution of skin friction along the shaft, the characteristics of the soil where the foundations will be built, the changes in the initial conditions caused by their execution, the complicated behavior of the pile-soil assembly, difficult to numerical or analytical modeling, support the need to use static load tests in foundations.

In caisson, static load tests aim to prove the element's ability to resist the axial load for which it was designed and to obtain detailed information on the settlements, to obtain values of skin friction resistance and bell resistance. In Brazil, static load tests are standardized by NBR 16903 (ABNT, 2020a), replacing NBR 12131 (ABNT, 2006) which can be applied to all types of piles, both vertical and inclined, regardless of the execution process and installation on the ground.

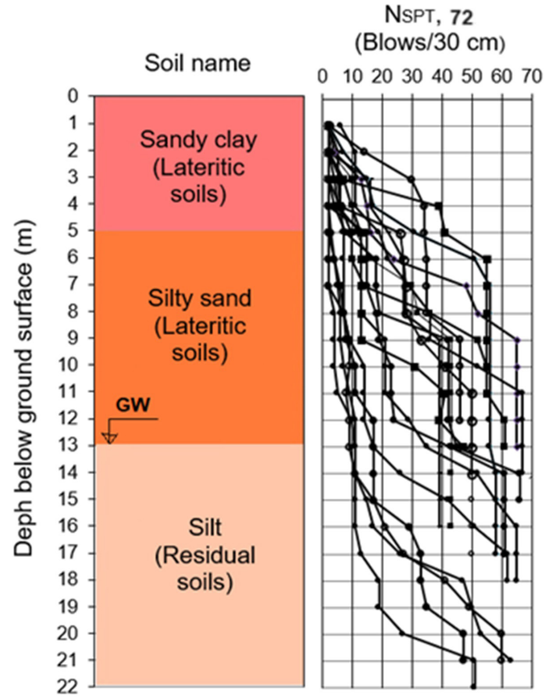

Figure 1. Soil profile of the study area.

2. Experimental study

In the Planalto Central, DF, Brazil region there is a notable predominance of residual porous lateritic silty clays, overlying a rocky mantle made up of quartzites, slates, phyllites and siltstones. The texture and mineralogical composition of these soils are a function of the underlying rock and weathering processes, such as laterization.

At the study site, twenty (20) Standard Penetration Test (SPT), were carried out, in accordance with NBR 6484 (ABNT, 2020b), to characterize the subsoil conditions. The soil stratigraphy is shown in Figure 1. A layer of red sandy clay (lateritic soil), very soft to soft, with a thickness of up to 5 m and N_{SPT} between 2 and 7 blows covers a large deposit of silty sand, with N_{SPT} values of up to 40 blows. The final layer is characterized by silty sand, interspersed with sandy silt, compact to very compact and N_{SPT} values greater than 45 blows (residual soil). The ground water was found at an average depth of 13 m below the surface.

For the experimental study, three (3) static load tests were carried out, identified as PC05, PC10 and PC11, in caisson with a shaft diameter of 0.6 m and bases of 1.2 m (PC10 and PC11) and 1.3 m (PC05).

For execution, a drill on a truck was used to excavate the shaft and widen the base manually. The concrete used for filling was 35 MPa. Figure 2 shows the distribution of static load tests in the study site, the depth at which the caissons were executed, and Figure 3 presents details of the type test caisson.

The reaction system included an iron beam anchored in two reaction caissons, with a shaft diameter of 1.0 m, without enlarging the bell, 2.65 m apart from axis to axis of the tested caisson, as shown in Figure 3. The lengths varied between 8 and 18 m, filled with 35 MPa concrete.

The two reaction caissons have INCOTEP brand anchors, type INCO 90D, throughout their entire length that function as traction elements, with the capacity to resist at least 50% of the maximum load predicted for the static load test, with a minimum distance between the reaction caissons, the system of caissons and tested caisson with three times (3x) the diameter of the largest cross-section, according to NBR 16903 (ABNT, 2020a).

To apply the load, a hydraulic jack with a capacity of 2000 kN was used. The applied load was read using a load cell with a capacity of 2000 kN. To read the displacements, six deflectometers were used, four at the top, diametrically opposed, and two on the sides, as shown in Figure 4.

The static load tests were carried out with reading loading (SML – Slow Maintained Load), in accordance with NBR 16903 (ABNT, 2020a). Albuquerque (2001) mentions in his paper that, even though the slow test (SML) requires a lot of time for its execution, the resulting load-displacement curve more adequately represents the behavior of the foundation at a given loading stage. For Velloso and Lopes (2002), the

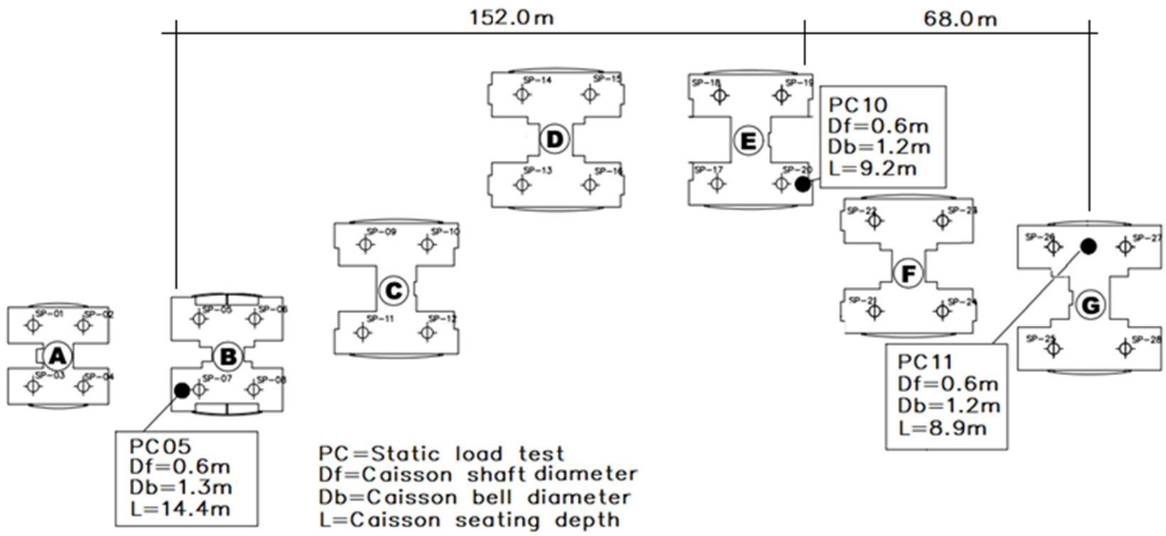

Figure 2. Distribution of static load tests at the study site.

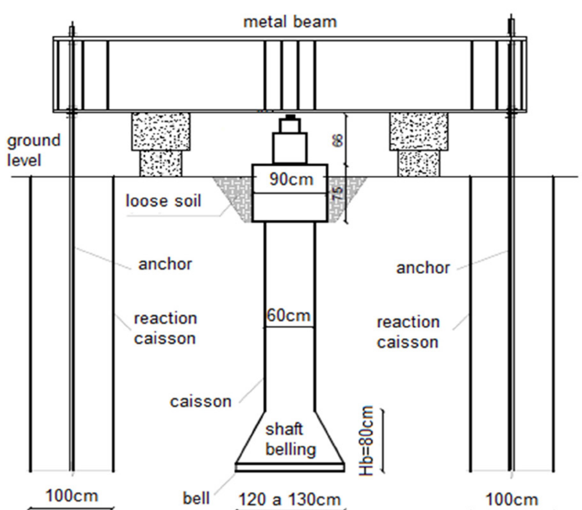

Figure 3. Layout of the static load test reaction system.

slow load (SML) is the one that best approximates the load to which the pile will be subjected under the future structure. According to the authors, when the soil is sheared quickly, it presents lower deformations and greater resistance due to its viscosity. As a result, longer loading stages, a lower loading speed leads to greater settlements and lower load capacities. Table 1 presents data on the static load tests performed.

The instrumentation of the caissons was carried out using a set of CA-50 steel bars, at different levels along the depth. The installed instrumentation consisted of electrical resistance strain gauges type KFG2 -120 – D16 -11 from Kyowa Eletronic Instruments CO. Ltd. glued to CA-50 steel bars, 1/2” in diameter and 0.4 m long and installed in pairs at the same level, in a diametrically opposite position, with a full bridge type connection between the strain gauges. The connections between the bars were made with a threaded system at the end of each bar alongside steel sleeves. To ensure the centralization of instrumentation in the caissons, steel centralizers were used at the tip of the caissons. To connect the instrumented bars to the reader unit, a 4 x 26 AWG electrical cable was used. The strain gages were protected against humidity and mechanical shocks using electrical insulation resin, silicone adhesive and adhesive tape. After placing the instrumented bar, concreting was carried out to consolidate the instrumented bar-caisson system. The instrumented bars were calibrated at UNICAMP, and this calibration aimed to make it possible to correct any differences in deformation readings and possible installation errors. After calibration, the bars were, during installation, joined using threads to form a continuous bar.

For the PC05 static load test, the levels were 0.2 m (reference section), 9.1 m and 13.8 m (located in the shaft) and 14.4 m (at the bell). For PC10, the levels were 1.0 m (reference section); 2.4 m; 5.1 m and 8.8 m (located in the shaft) and 9.2 m (at the bell). For PC11, the levels were 1.0 m (reference section); 2.3 m and 5.2 m (located in the shaft) and 8.9 m (at the bell).

3. Analysis and results

Figure 5 to Figure 7 presents the results obtained by the instrumentation during the static load tests. To analyze the instrumentation, the modulus of elasticity obtained in the reference section of the caisson (extensometer positioned at the top of the caisson) was adopted, using stress-strain curves according to deformation ranges and the Fellenius (2023) methodology.

For PC05, with a total load of 1964 kN, a maximum load of 1804 kN was transferred to the instrumented shaft,

Table 1. Data on the static load tests performed on caissons.

Static load test	Caisson			Working load (according to the project)	Maximum load test	Total displacement
	Depth	Shaft	Bell			
	(m)	(cm)	(cm)	(kN)	(kN)	(mm)
PC5	14.4	60	130	982	1963	6.29
PC10	9.2	60	120	981	1962	6.97
PC11	8.9	60	120	982	1964	11.47

(a) (b)

Figure 4. a) general view; b) detailed view.

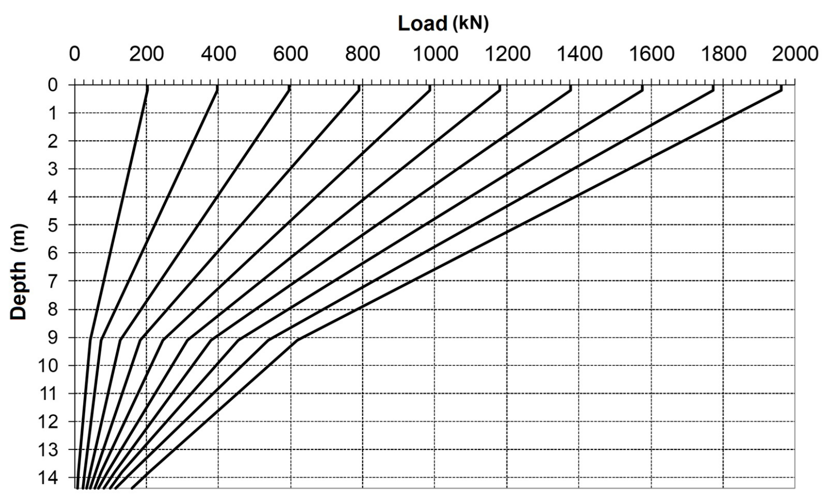

Figure 5. Load transfer along the shaft and bell of the caisson – PC05.

equivalent to 91.9%, the difference being 8.1% absorbed by the bell. The mobilization of the bell of the caisson in the first loading (202 kN) is equivalent to 4.4% of the total load applied in that stage. For the other load stages, the values were in the order of 5.6% to 6.5%, reaching a maximum value of 8.1% in the last stage.

In the case of the PC10 load test, the total load was 1992 kN, transferring a maximum load of 1496 kN to the instrumented shaft, equivalent to 76.2%. The load measured at a depth of 9.2 m was 467 kN equivalent to 23.8%. There was mobilization of the bell of the caisson from the first loading (199 kN) with values of the order of 14 kN equivalent to 7.0%, reaching a maximum value of 23.8% in the last stage.

For PC11, the total load was 1964 kN, transferring a maximum load of 722 kN to the instrumented shaft, equivalent to 36.8%. The load measured at a depth of 8.9 m was 1242 kN equivalent to 63.2%. There was mobilization of the bell of the caisson from the first loading (204 kN) with values of around 48 kN equivalent to 23.8%, reaching a maximum value of 63.2% in the last stage.

To analyze the instrumented static load tests, the finite element Plaxis 3D software was used, developed for

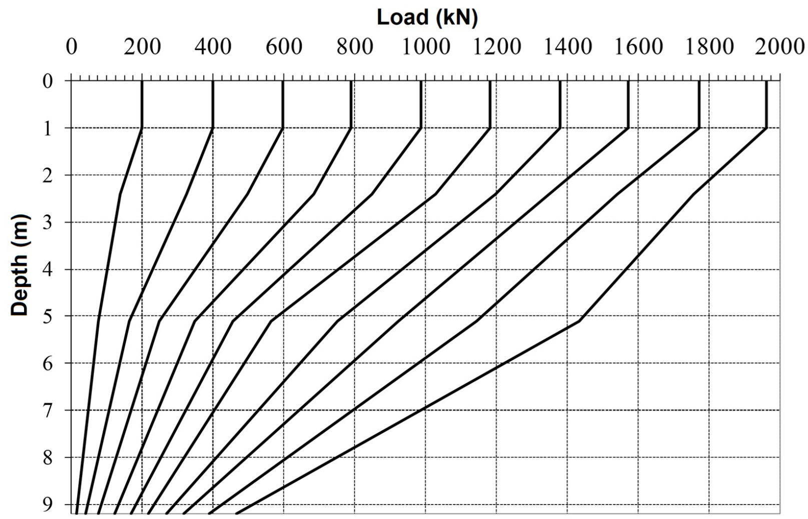

Figure 6. Load transfer along the shaft and bell of the caisson – PC10.

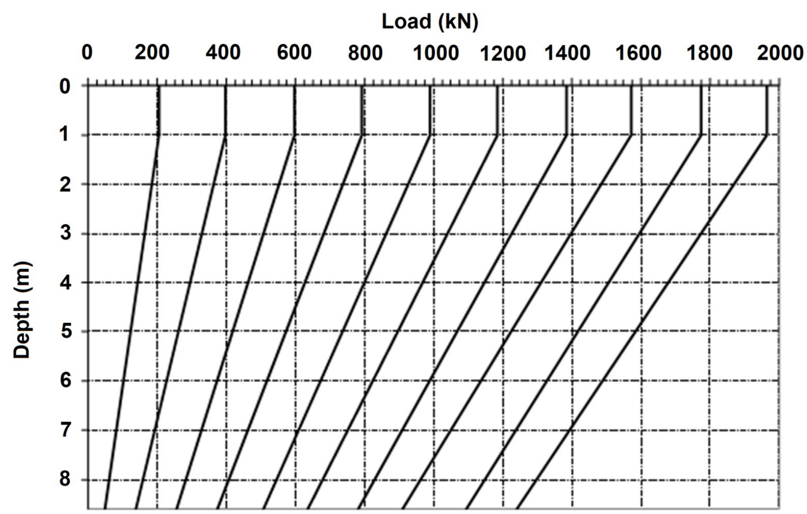

Figure 7. Load transfer along the shaft and bell of the caisson – PC11.

analyzing deformations, stability, and ground water level in geotechnical engineering. For the numerical simulation, the perfectly plastic Mohr-Coulomb linear elastic model was used, with the main input parameters: elastic modulus (E), Poisson's ratio (v), friction angle (ϕ), cohesion (c) for soil plasticity and soil specific weight (γ). This Mohr-Coulomb model represents a "first order" approximation of soil or rock behavior. Soil parameters were determined by empirical correlations with N_{SPT} values from Table 2 of Joppert Jr. (2007). These parameters were used as initial input data within the Plaxis 3D software.

Then, back-calculations were carried out, with variation of soil parameters, to arrive at an approximation of the load vs displacement curve presented in the static load tests. For the concrete of the caissons, the linear elastic model was used, which is based on Hooke's Law, of isotropic elasticity, which involved the input elastic parameters: the modulus of elasticity (E_c) = 35000 MPa, the Poisson's ratio (v) = 0,20 and the specific weight of the concrete (γ_c) = 25 kN/m^3. Table 3 shows the parameters resulting from the back-calculations of the Plaxis 3D software.

Figure 8 to Figure 10 presents the curves vs displacements resulting from the back-calculation.

The load vs displacement curves using the Plaxis 3D software showed conventional rupture displacements, with continued deformations following new load increases. According to NBR 6122 (ABNT, 2022), this behavior of the load vs displacement curve occurs in the following circumstances: when there is a limitation of the reaction load, or the load capacity of the caisson is greater than the applied load and when the caisson is loaded until it presents high displacements without a clear rupture configuration.

Table 2. Average geotechnical parameters of soils (adapted, Joppert Junior, 2007).

Soil	NSPT	E (MPa)	Specific weight		ϕ (°)	c (kPa)
			γ (kN/m³)	γ_{sat} (kN/m³)		
Slightly silty sand/ Lightly clayey sand	0-4	20-50	17	18	25	-
	5-8	40-80	18	19	30	-
	9-18	50-100	19	20	32	-
	19-41	80-150	20	21	35	-
	>=41	160-200	20	21	38	-
Medium sand and very clayey fine sand	0-4	20	17	18	25	0
	5-8	40	18	19	28	5
	9-18	50	19	20	30	7.5
	19-41	100	20	21	32	10
Red and yellow porous clay	0-2	2-5	15	17	20	7.5
	3-5	5-10	16	17	23	15
	6-10	10-20	17	18	25	30
	>=10	20-30	18	19	25	30 to 70
Slightly sandy silty clay (tertiary soil)	0-2	1	17	18	20	7.5
	3-5	1-2.5	18	19	23	15
	6-10	2.5-10	19	19	24	20
	11-19	5-10	19	19	24	30
	20-30	30-100	20	20	25	40
	>=30	100-150	20	20	25	50
Lightly silty sandy clay	0-2	5	15	17	15	10
	3-5	5-15	17	18	15	20
	6-10	15-20	18	19	18	35
	11-19	20-35	19	19	20	50
	>=20	35-50	20	20	25	60
Turf/ Organic clay	0-1	0.4-1	11	11	15	5
	2-5	1-5	12	12	15	10
Lightly clayey sandy silt (residual soil)	5-8	8	18	19	25	15
	9-18	10	19	20	26	20
	19-41	150	20	20	27	30
	>=41	200	21	21	28	50

Table 3. Geotechnical design parameters of the caissons resulting from the back-calculations of the Plaxis 3D.

Static load test	Soil type	Material Model	Drainage type	γ (kN/m³)	γ_{sat} (kN/m³)	c (kPa)	ϕ (°)	E (MPa)	ν
PC05	Sandy Clay	Mohr-Coulomb	Drained	17	18	22	15	15	0.30
	Compact silty sand	Mohr-Coulomb	Drained	19	19	30	18	18	0.30
	Clayey silt	Mohr-Coulomb	Drained	20	21	40	25	24	0.30
PC10	Sandy Clay	Mohr-Coulomb	Drained	17	18	22	15	15	0.30
	Silty sand	Mohr-Coulomb	Drained	19	19	32	28	40	0.30
	Sandy silt	Mohr-Coulomb	Drained	20	21	45	28	60	0.30
PC11	Sandy Clay	Mohr-Coulomb	Drained	17	18	22	15	15	0.30
	Silty sand	Mohr-Coulomb	Drained	19	19	32	28	34	0.30
	Sandy silt	Mohr-Coulomb	Drained	20	21	40	28	60	0.30
Caisson	Concrete	Linear elastic	Non-porous	25	-	-	-	35000	0.20

Legend: Weight (γ); saturated specific weight (γ_{sat}); Cohesion (c); Soil friction angle (ϕ); Elastic Modulus E; Poisson's ratio (ν).

In these cases, the interpretation of the caisson load tests configured conventional rupture in all cases. The loading speed, stabilization of displacements and the nature of the terrain are considerations raised that affect the results of load tests for cases of conventional ruptures as recommended by NBR 12131 (ABNT, 2006).

The small displacements configured at the beginning of loading up to the limit of the static test load demonstrate that

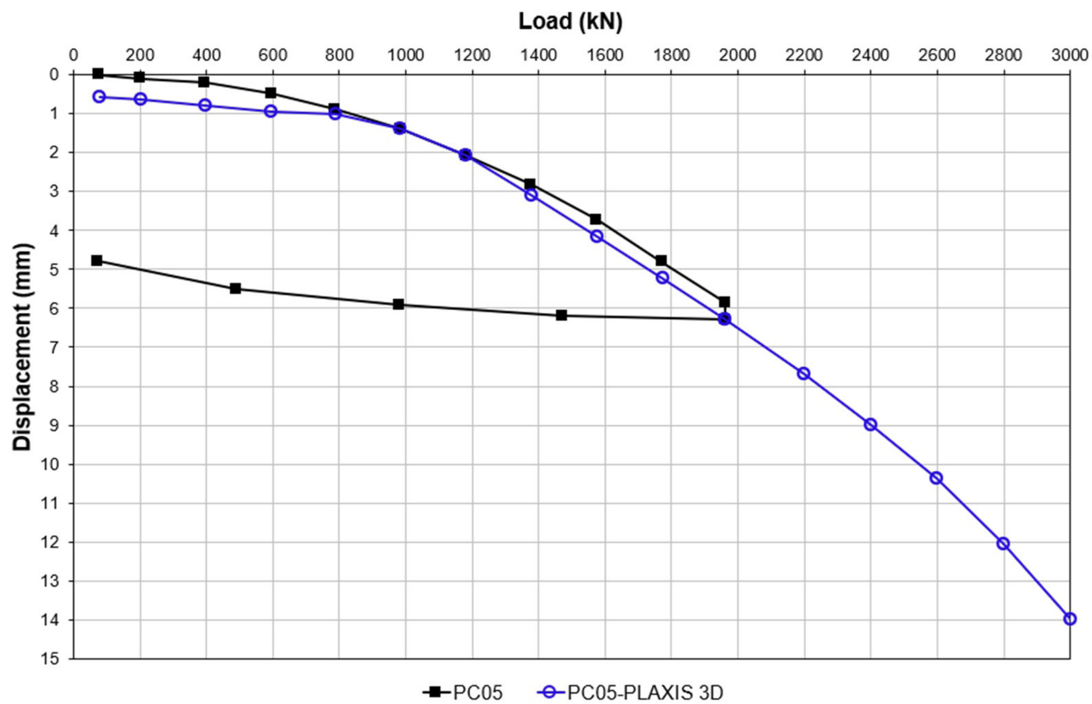

Figure 8. Back-calculation of the load vs displacement curve in the PLAXIS 3D – PC05.

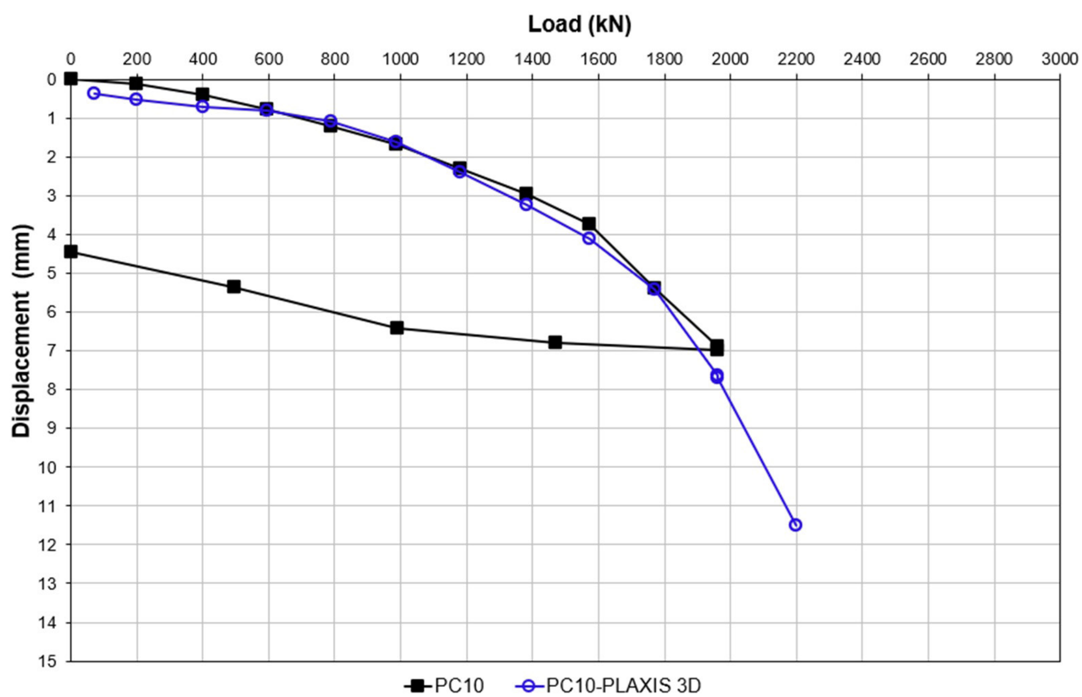

Figure 9. Back-calculation of the load vs displacement curve in the PLAXIS 3D – PC10.

there is a significant load being mobilized by skin friction along the axis of the caissons for PC05, PC10 and PC11. Given that the working load is between 981 kN and 982 kN, the initial displacements that occurred were mobilized by the skin friction portion at the beginning of the linear-elastic deformation of the displacement curve.

The result of the PC05 instrumentation shows that the length of the caisson has a significant contribution to the

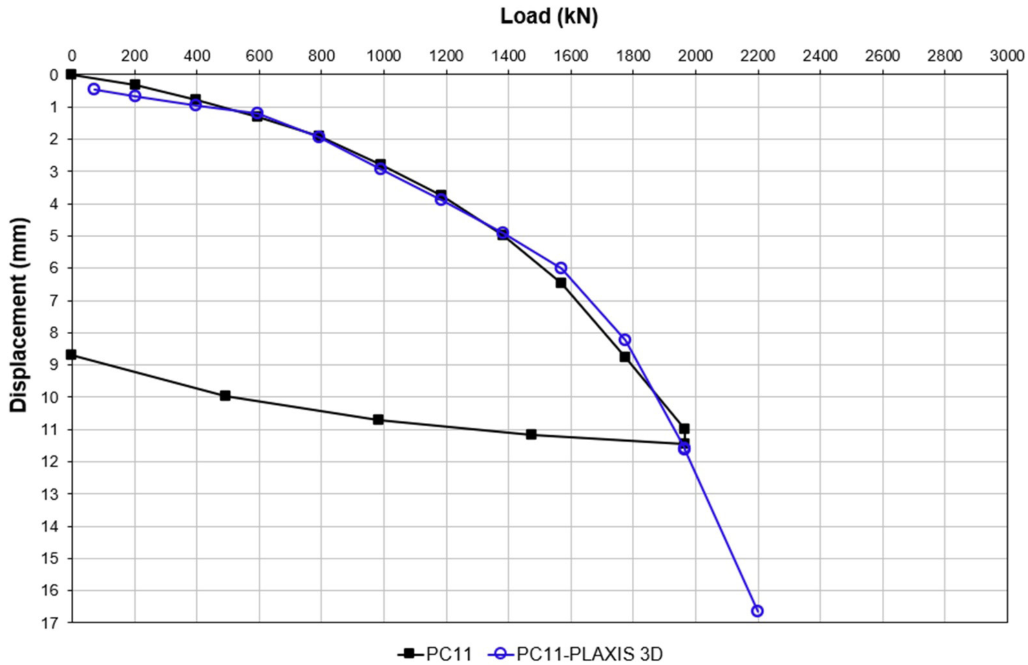

Figure 10. Back-calculation of the load vs displacement curve in the PLAXIS 3D – PC11.

mobilization of skin friction, since a small portion of the load was mobilized at the bell. For PC10 and PC11, the skin friction load had a smaller contribution due to the length of the caissons, however, this portion must be considered when analyzing the behavior of the caissons for tropical soils of the same geological feature.

In the paper of Pereira & Garcia (2023) an extensive study was carried out on the contribution of resistance to skin friction in caissons and confirms that the load capacity of caissons has a significant increase when the portion of resistance to skin friction is considered.

In instrumented static load tests, based on the methodology of Camapum de Carvalho et al. (2008, 2010), soil mobilization at the interface with the foundation and plasticization of the entire complex were evaluated.

The methodology proposed by Camapum de Carvalho et al. (2008, 2010), analyzes the settlement/displacement coefficient (α) plotted in relation to the loads and is based on the laboratory consolidation test. The coefficients are extracted from the graph plotted on a logarithmic scale, in a similar treatment to the consolidation test, for each load, from the linear final part of the settlement curves (mm) as a function of time.

The resulting graph presents three straight segments, where the 1st section defines the beginning of the plastic deformations of the shaft-soil system, that is, the friction domain. The 2nd section is characterized by mobilization of the tip and the 3rd represents the beginning of plastic deformations of the soil at the tip of the pile (Figure 11).

From the results of the static load tests, it was possible to obtain graphs in terms of ultimate settlement, measured as a function of the applied load. Figure 12, Figure 13 and Figure 14 show the accumulated immediate settlements and accumulated settlements due to consolidation and/or secondary, depending on the applied loads, for the load tests. The curves indicate the changes in the behavior of the caissons.

The mobilization of the skin friction of the caisson begins up to the 1st point of intersection, suffering small settlements with the applied load. From this load onwards, the shaft and bell of the coffin begins to work in an integrated manner, with the beginning of the mobilization of the tip, which is preponderant in relation to the load to which the foundation is subjected. The 2nd intersection point with the 3rd section corresponds to the beginning of plastic deformations of the soil at the base of the foundation, however, it does not mean the occurrence of rupture but rather that, from this point onwards, the settlements become more relevant.

Analyzing the graphs presented in Figure 12, Figure 13 and Figure 14, four Intersections are indicated that show the behavior of the foundation, as shown in Table 4.

Intersection 1 – Load with which work on the shaft begins (with few settlements occurring).

Intersection 2 – Value at which the contribution of the shaft and bell set begins in an integrated manner up to the indicated load.

Intersection 3 - In the accumulation and/or secondary settlements accumulated due to the loads applied to the caisson, it was observed that the shaft begins to work with small settlements until close to the indicated load.

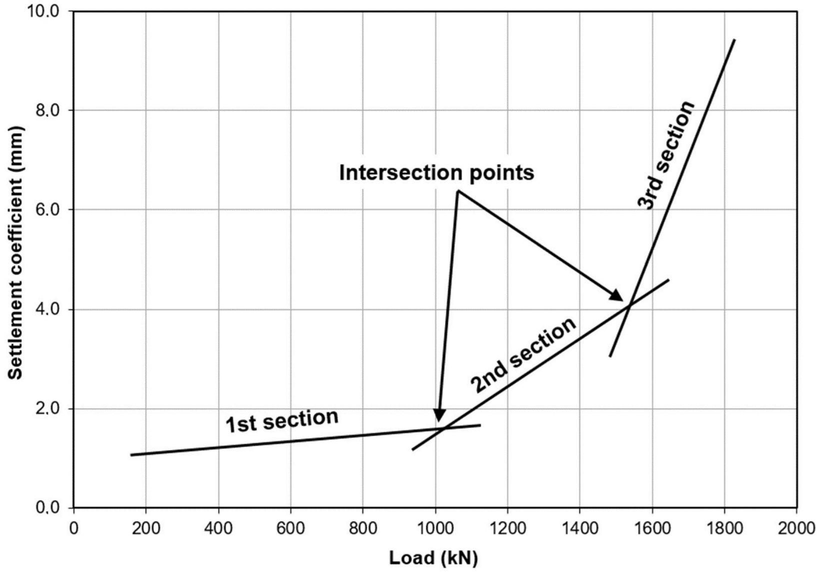

Figure 11. Load vs settlement coefficient (Camapum de Carvalho et al., 2010).

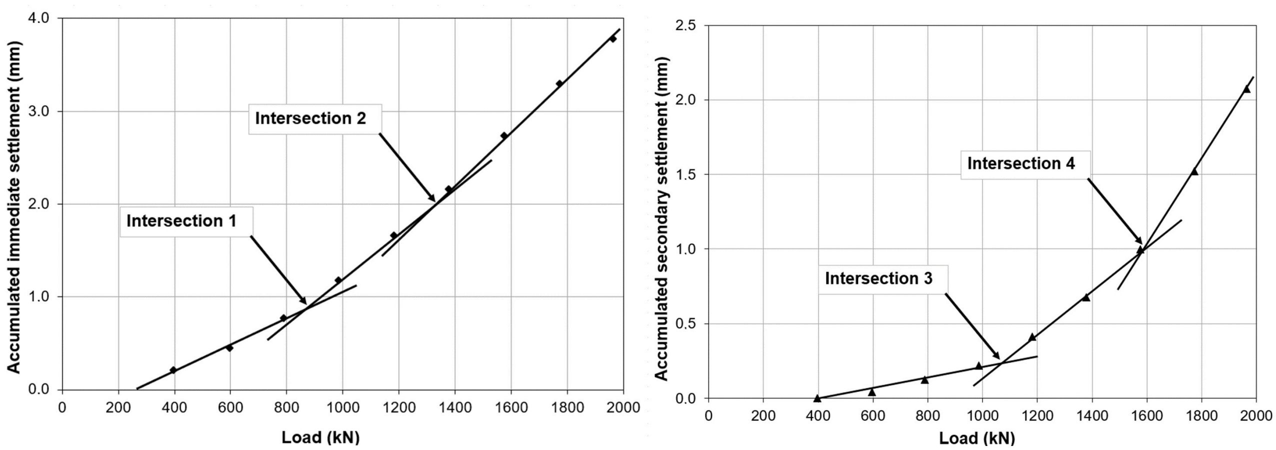

(a) (b)

Figure 12. Curves load vs accumulated immediate settlement (a) and load vs accumulated secondary settlement (b) – PC05.

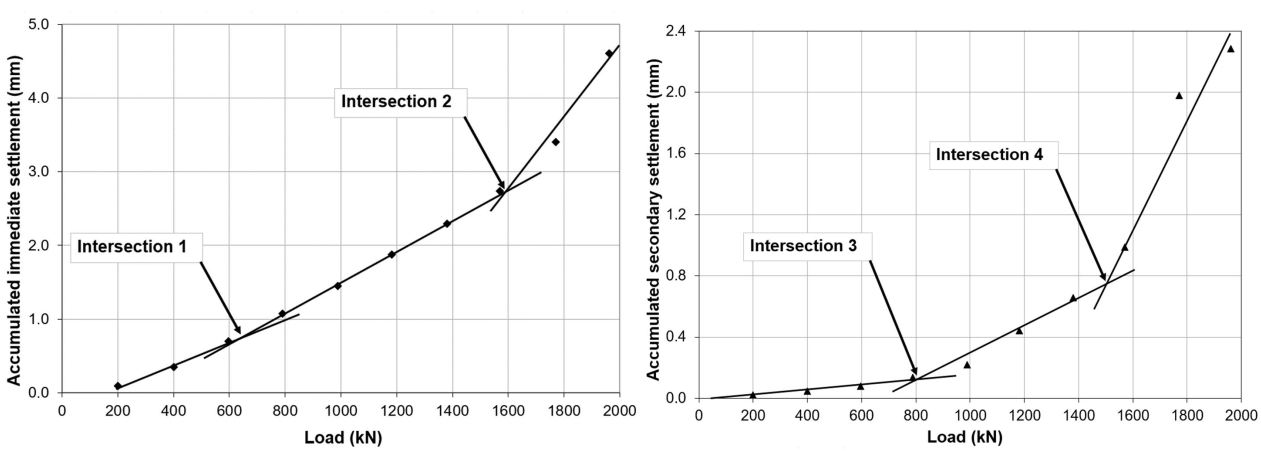

(a) (b)

Figure 13. Curves load vs accumulated immediate settlement (a) and load vs accumulated secondary settlement (b) – PC10.

Table 4. Loads identified in the loading phases.

Static load test	Intersection 1	Intersection 2	Intersection 3	Intersection 4
PC 05	870 kN	1380 kN	1070 kN	1580 kN
PC 10	640 kN	1590 kN	800 kN	1510kN
PC 11	840 kN	1410 kN	990 kN	1570 kN

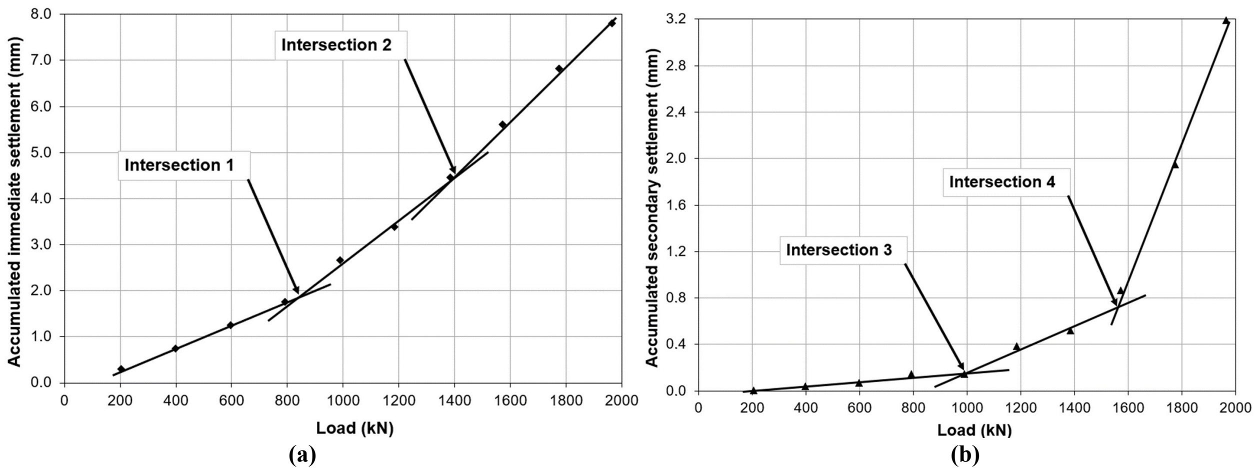

Figure 14. Curves load vs accumulated immediate settlement (a) and load vs accumulated secondary settlement (b) – PC11.

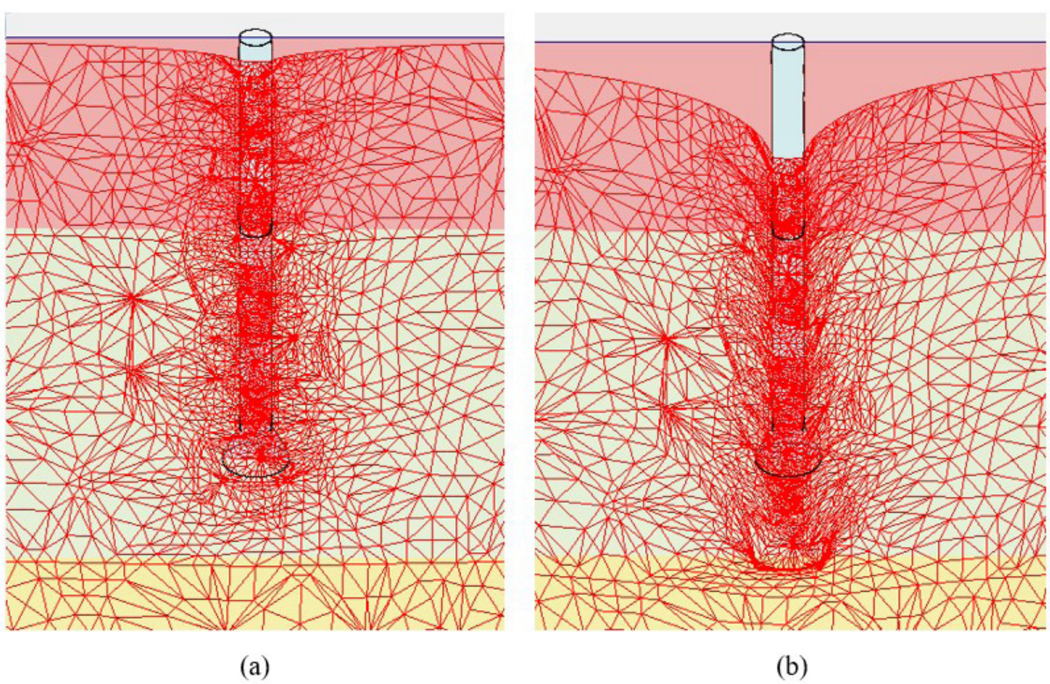

Figure 15. Numerical analysis of loads in Plaxis 3D. a) Mobilization of the shaft; b) shaft+bell mobilization.

Intersection 4 - After the load indicated in Intersection 3, the shaft and bell set compete in an integrated manner until approximately the indicated load.

From the back-calculation that validated the numerical model for analyzing the behavior of the caissons, it was possible to identify when the mobilization of skin friction occurs and when the mobilization of loads towards the bell of the caissons begins. In Figure 15 it is possible to see the beginning of these mobilizations using Plaxis 3D software. Table 5 shows the loads identified in the loading phases in Plaxis 3D.

To determine the skin friction load and initiate the mobilization of the load in the caisson bell for the Plaxis

Table 5. Loads identified in the loading phases in the Plaxis 3D.

Static load test	Resistence shaft	Resistence shaft+ resistence bell
PC 05	788 kN	1575 kN
PC 10	596 kN	1381 kN
PC 11	597 kN	1185 kN

3D software, the reductions in displacement increments were analyzed with the application of the load in each loading phase. It was noted that from the 3rd loading phase onwards (approximately 596 kN and 597 kN) for load tests PC10 and PC11, the displacements undergo small and constant increments, which indicates the beginning of load mobilization at the bell. For PC05 this only occurs in the 4th loading phase due to the length of the caisson shaft (14.4 m). As the caisson is considered a rigid reinforced concrete element in the simulations, soil mobilization is clear, both in the shaft and at the bell of the caisson, as shown in Figure 15.

The instrumentation results for load tests PC05, PC10 and PC11 indicate that from the 1st load the load mobilization on the bell begins. For PC10 and PC11, total mobilization of the shaft occurs for loads of 1496 kN and 1242 kN respectively, which corresponds to the 2nd point of intersection according to the methodology of Camapum de Carvalho et al. (2008, 2010), where the bell mobilization begins. For PC05, the maximum skin friction load was 1804kN, which indicates that the length of the caisson directly affects the mobilization of skin friction.

In the Plaxis 3D results, the total mobilization of skin friction occurs between the 3rd and 4th loads, with mobilization of the bell starting from the 6th and 7th loads.

Given the results of the instrumented load tests PC05, PC10 and PC11 and Plaxis 3D, the set of analyzes allowed us to verify that the Camapum de Carvalho et al, methodology. (2008, 2010) presents good accuracy, identifying the region dominated by skin friction, bell and plasticization of the foundation.

4. Conclusion

The results of the in-depth instrumentation of the caissons show a significant contribution from the portion of skin friction resistance developed for a fraction of the displacement necessary to mobilize the resistance, which should be considered in the analysis of the behavior of open pit caissons for soils of the same characteristic from the Planalto Central, DF, Brazil.

With the results of the static load tests, it was also observed that increasing the bell by up to two times (2x) the shaft diameter contributes significantly to the increase in resistance or decrease in displacement. The resistance to skin friction has a constant value, with the proportion of load decreasing as the bell increases. This means that in caissons, the rupture of the bell has no practical definition, as the displacement necessary for their mobilization is excessive and the structures would not support such displacements for their complete mobilization.

When comparing the results obtained by the method of Camapum de Carvalho et al. (2008) and the Plaxis 3D software, it can be stated that the loads are close together, confirming the methodology proposed by numerical methods and the authors' predictions for a tropical soil in the Distrito Federal. Therefore, the method constitutes an important tool for analyzing the loads mobilized along the shaft and bell of the caissons.

It is important to highlight that the analysis of the results is not restricted to determining the load capacity, but goes further, establishing the domains of friction, tip and plastification, information that is difficult to measure and preponderant in the design of foundations, especially in non-static load tests led to failure.

Acknowledgements

We thank the Universidade Estadual de Campinas – UNICAMP for the opportunity to develop research.

Declaration of interest

The authors have no conflicts of interest to declare. All co-authors have observed and affirmed the contents of the paper and there is no financial interest to report.

Authors' contributions

Regina Maria Ferreira: conceptualization, methodology, validation, resources, software, writing – original draft. Paulo Jose Rocha de Albuquerque: formal analysis, data analysis, supervision, validation, writing – review & editing. Neusa Maria Bezerra Mota: formal analysis, methodology, supervision, validation.

Data availability

The datasets generated analyzed in the course during of the current study are available from the corresponding author upon request.

List of symbols and abbreviations

3D	Three-dimensional modeling
c	Cohesion
ABNT	Brazilian Association of Technical Standards
E	Elastic Modulus
E_c	Elastic Modulus of concrete
NBR	Brazilian standard
SPT	Standard Penetration Test
SML	Slow Maintained Load

UNICAMP Universidade Estadual de Campinas
γ Weight
γ_c Specific weight of the concrete
γ_{sat} Saturated specific weight
ν Poisson's ratio
ϕ Soil friction angle

References

ABNT NBR 12131 (2006). *Solo – estacas - prova de carga estática – Método de ensaio*. ABNT - Associação Brasileira de Normas Técnicas, Rio de Janeiro, RJ (in Portuguese).

ABNT NBR 16903 (2020a). *Solo - Prova de carga estática em fundação profunda*. ABNT - Associação Brasileira de Normas Técnicas, Rio de Janeiro, RJ (in Portuguese).

ABNT NBR 6122 (2022). *Projeto e Execução de Fundações*. Associação Brasileira de Normas Técnicas, Rio de Janeiro, RJ (in Portuguese).

ABNT NBR 6484 (2020b). *Solo - Sondagens de simples reconhecimentos com SPT – Método de ensaio*. ABNT - Associação Brasileira de Normas Técnicas, Rio de Janeiro, RJ (in Portuguese).

Albuquerque, P.J.R. (2001). *Estaca escavadas, hélice contínua e ômega: estudo do comportamento à compressão em solo residual de diabásio, através de provas de carga instrumentadas em profundidade* [Doctoral thesis]. Escola Politécnica, Universidade de São Paulo. (in Portuguese).

Berberian, D. (2017). *Engenharia de Fundações* (33. ed.). Editora da Universidade de Brasília. (in Portuguese).

Bowles, J.E. (1997). *Foundation Analysis and Design* (5th ed.). Editora McGraw Hill, Inc.

Brown, D.A., Turner, J.P., Castelli, R.J., & Loehr, E.J. (2018). *Drilled shafts: construction procedures and design methods*. Federal Highway Administration.

Camapum de Carvalho, J., Silva, C.M., Aquino, F.R., Aguiar, L.A., Mota, N.M.B., & Albuquerque, P.J.R. (2010). Análises dos resultados de provas de carga estáticas sobre fundações profundas. In: *COBRAMSEG, 2010 - Engenharia Geotécnica para o Desenvolvimento: Inovação e Sustentabilidade* (pp. 01-08). São Paulo: ABMS. (in Portuguese).

Camapum de Carvalho, J., Silva, C.M., Paolucci, H.V.N., González, Y.V., & Valencia, L.A.L. (2008). Considerações sobre à análise dos resultados de provas de carga estáticas. In: *Seminário de Engenharia de Fundações Especiais e Geotecnia* (p. 355-369). São Paulo: ABMS. (in Portuguese).

Castro Neto, J.R., Faustino, C.L., & Albuquerque, P.J.R. (2019). Avaliação da Transferência de Carga em Profundidade de Estacas Hélice Contínua com Base no Conceito do Adensamento Unidimensional. In: *Seminário de Engenharia de Fundações Especiais e Geotecnia* (pp. 1-9). São Paulo: ABMS. (in Portuguese).

Das, M.B. (2016). *Principles of Foundation Engineering* (8th ed.). Cengage Learning.

Fellenius, B.H. (2023). *Basic of Foundation Design*. Retrieved in October 9, 2023, from www.fellenius.net/papers/428%20The%20Red%20Book,%20Basics%20of%20Foundation%20Design%202023.pdf

Herrmann, R.A., Löwen, M., Tinteler, T., & Krumm, S. (2013). Research on the Load-Bearing Behavior of Bored Piles with Different Enlarged Bases. In: *18th International Conference on Soil Mechanics and Geotechnical Engineering* (pp. 2755-2758). London: International Society of Soil Mechanics and Geotechnical Engineering.

Johnson, L.D., Sherman, W.C., & Al-Hussaini, M.M. (1981). *Overview for design and construction of drilled shafts in cohesive soils.* Geotechnical Laboratory. U. S. Army Engineer Waterways Experiment Station.

Joppert Junior, I. (2007). *Fundações e contenções de edifício: qualidade total na gestão do projeto e execução*. Pini. (in Portuguese).

Murthy, V.N.S. (2002) *Geotechnical Engineering: principles and practices of soil mechanics and foundation engineering*. New York: Marcel Dekker Inc.

Pereira, B.E., & Garcia, J.R. (2023). Numerical analysis of the contribution of side resistance to caisson bearing capacity. *Soils and Rocks*, 46(2), e2023000123.

Silva, C.M. (2011). *Energia e confiabilidade aplicadas aos estaqueamentos tipo hélice contínua* [Doctoral thesis]. Departamento de Engenharia Civil e Ambiental, Universidade de Brasília. (in Portuguese).

Velloso, D.A., & Lopes, F.R. (2002). *Fundações profundas* (vol. 2, 359 p.). Rio de Janeiro: Coppe – UFRJ.